

Chiral anomaly: from vacuum to Columbia plot

Francesco Giacosa^{a,b}, Győző Kovács^{c,d}, Péter Kovács^d, Robert D. Pisarski^e and Fabian Rennecke^{f,g}

^a*Institute of Physics, Jan Kochanowski University, ulica Uniwersytecka 7, Kielce, P-25-406, Poland*

^b*Institute for Theoretical Physics, Goethe-University, Max-von-Laue-Straße 1, Frankfurt am Main, D-60438, Germany*

^c*University of Wrocław, Plac Maxa Borna, Wrocław, 50204, Poland*

^d*HUN-REN Wigner Research Centre for Physics, Konkoly-Thege Miklós ut 29-33, Budapest, 1121, Hungary*

^e*Department of Physics, Brookhaven National Laboratory, Plac Maxa Borna, Upton, NY, 11973, USA*

^f*Institute for Theoretical Physics, Justus-Liebig University Giessen, Heinrich-Buff-Ring 16, Giessen, 35392, Germany*

^g*Helmholtz Research Academy Hesse for FAIR (HFHF), Campus Giessen, Giessen, 35392, Germany*

ARTICLE INFO

Keywords:
chiral anomaly
polydeterminant
Columbia plot
chiral models
eLSM

Abstract

We use a low-energy effective approach, the extended linear sigma model, to study realizations of the $U(1)_A$ anomaly with different operators, linear and quadratic in the 't Hooft determinant. After discussing the parameterization in agreement with vacuum's phenomenology, we investigate the influence of these different anomaly terms on the Columbia plot: the square of the 't Hooft determinant favors a cross-over for small quark masses. Finally, we also discuss the extension of the 't Hooft determinant to cases in which different mesonic multiplets interact with each other. Novel chiral anomalous interaction terms involving excited (pseudo)scalar states, pseudovector, and pseudotensor mesons are expressed via a mathematical extension of the determinant, denoted as a *polydeterminant*.

1. Introduction

The chiral (or axial) anomaly is an important feature of Quantum Chromodynamics (QCD): this $U(1)_A$ symmetry of the classical Lagrangian in the chiral limit (the limit in which the bare quark masses vanish) is broken by gluonic quantum fluctuations.

It is well known that the chiral anomaly has an important impact on vacuum physics: the mass of the $\eta'(958)$ meson receives a large contribution, making it not a quasi-Goldstone boson, not even in the chiral limit [1, 2]. In turn, this anomaly is also responsible for the very good realization of isospin symmetry at the level of the pions [3, 4]. (For a recent unexpected breaking of isospin symmetry far beyond expectations, see Refs. [5, 6].)

The effective description of the chiral anomaly in the vacuum takes place via suitable determinant-like terms [1, 2, 7, 8]. In fact, the determinant is tailor-made to preserve $SU(3)_L \times SU(3)_R$ chiral symmetry but to break the $U(1)_A$ classical axial symmetry, reflecting the QCD chiral (or axial) anomaly. In Sec. 2.1 we recall how these features are implemented in the context of the extended linear sigma model with (axial-)vector mesons (eLSM, see e.g. Refs. [9, 10]). In particular, we consider an additional term proportional to the square of the usual 't Hooft determinant. Next, in Sec. 2.2 we describe the vacuum parametrization of these anomaly terms in agreement with the constraints provided by vacuum physics (masses and decays listed in the PDG [11]). Besides these determinant terms, in Sec. 2.3 we discuss other anomalous interactions are possible by using a generalization of the determinant, named polydeterminant in Ref. [12]. This

object allows to introduce interaction terms for distinct chiral multiplets and for glueball states.

The chiral anomaly is also important at nonzero temperature T , since it may affect the order of the chiral phase transition. For this reason, it was extensively studied in the past, e.g. Refs. [3, 13–16] and refs therein. Recently, in Ref. [17] under general terms and in Ref. [18] within the eLSM as a concrete approach, the role of the previously mentioned chiral anomalous terms was studied, in particular in connection with the Columbia plot. To this end, we recall that for three massless quark flavors (origin of the Columbia plot), a first-order transition has been predicted irrespective of the fate of $U(1)_A$ [15]. In lattice QCD, a second-order transition for $N_f \leq 6$ massless quark flavors is obtained [19]. For $N_f = 3$, other results determine stringent upper bounds for critical pion masses for second-order transition [20–22], see also Dyson-Schwinger second-order outcome of Ref. [23]. Here, we show how the novel anomalous term, the square of the 't Hooft determinant, strongly affects the Columbia plot, enlarging the cross-over region. The status is summarized in Sec. 3, where a different implementation of the Columbia plot than in Ref. [18] is shown.

Finally, in Sec. 4 we conclude and present some outlooks.

2. Anomalous interactions and the parametrisation

2.1. 't Hooft anomaly terms within the eLSM

In this work, we use the eLSM introduced for $N_f = 2+1$ in Refs. [9, 24] and applied at nonzero temperature and chemical potential in Refs. [25, 26]. For a recent review, see [10]. Continuing the work of Ref. [18], we discuss the effect of different $U(1)_A$ anomalous terms on the vacuum's parametrization and on the Columbia plot, while highlighting different aspects of our results.

*Contribution to XQCD 2025 Wrocław

✉ francesco.giacosa@ujk.edu.pl (F. Giacosa)

ORCID(s): 0000-0003-3735-7620 (F. Giacosa); 0000-0003-3735-7620 (Gy. Kovács); 0000-0003-3735-7620 (P. Kovács); 0000-0003-3735-7620 (R.D. Pisarski); 0000-0003-3735-7620 (F. Rennecke)

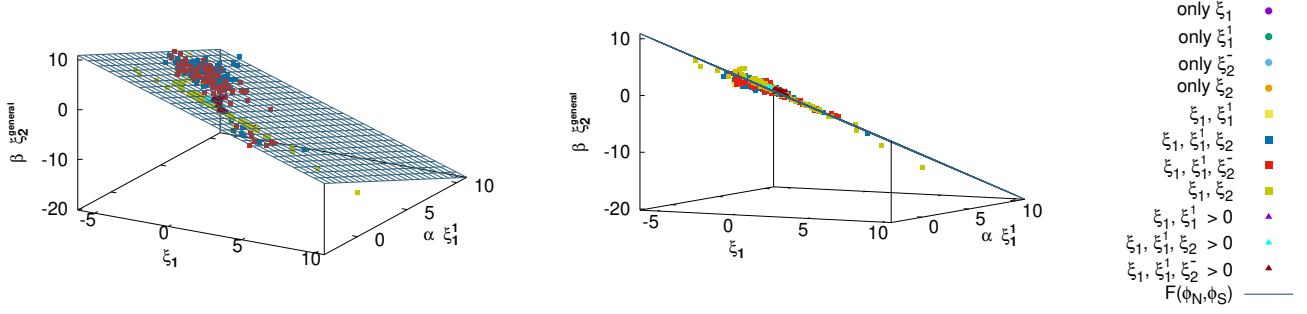


Figure 1: The different parameter sets in the parameters subspace spanned by the ξ_1 , ξ_1^1 , and $\xi_2^{\text{gen}} = \xi_2, \xi_2^{\pm}$ are aligned on the $F(\phi_N, \phi_S)$ surface $\xi_1 + \alpha \xi_1^1 + \beta \xi_2^{\text{gen}} = \bar{\xi}_{\text{eff}}$ determined by the constraint in Eq. (3). The numerical values are $\alpha = (0.13^2 + 0.14^2)/2$ and $\beta = 0.13^2 \cdot 0.14/\sqrt{2}$, while $\bar{\xi}_{\text{eff}} = 1.4$ is used, but it is not fixed during the parametrization procedure.

The Lagrangian of the eLSM is expressed in terms of a (pseudo)scalar field Φ (that contains pions, kaons, $\eta_{N,s}$ and their scalar chiral partners) as well as (axial-)vector fields. Under $SU(3)_L \times SU(3)_R$ chiral transformations, $\Phi \rightarrow U_L \Phi U_R^\dagger$, where $U_{L/R}$ are special unitary matrices. This transformation is called heterochiral [27].

The Lagrangian includes a classical chirally invariant part \mathcal{L}_{cl} and additional terms that account for the explicit symmetry breaking \mathcal{L}_{ESB} and the axial anomaly \mathcal{L}_{qu} . The term \mathcal{L}_{ESB} is simply given by $\mathcal{L}_{\text{ESB}} = \text{tr}(H\Phi)$, which gives rise to $h_N \phi_N + h_S \phi_S$ when the fields are taken to their nonstrange and strange vacuum expectation values, ϕ_N and ϕ_S respectively. For the term \mathcal{L}_{qu} , multiple operators satisfy the expected symmetry properties. Generally, one can write

$$\begin{aligned} \mathcal{L}_{\text{qu}} = & -\xi_1 (\det \Phi + \det \Phi^\dagger) \\ & - \xi_1^1 \text{tr}(\Phi^\dagger \Phi) (\det \Phi + \det \Phi^\dagger) \\ & - \xi_2 [(\det \Phi)^2 + (\det \Phi^\dagger)^2]. \end{aligned} \quad (1)$$

The first term is the mesonic 't Hooft determinant related to fluctuations of field configurations with topological charge $Q = 1$ [28]. The second term mixes anomalous and classical invariant contributions. The last, sixth-order term is generated by fluctuations with $Q = 2$ [29]. Instead of this term, one can use either of

$$\mathcal{L}_{\text{qu}}^{Q=2, \pm} = -\xi_2^\pm [(\det \Phi) \pm (\det \Phi^\dagger)]^2, \quad (2)$$

which differs only by a non-anomalous $\sim \det \Phi \det \Phi^\dagger$ invariant contribution. While the Lagrangian in Eq. (1) is the most general anomalous contribution with mass dimension $d_m \leq 6$ operators, for completeness, we investigate the parametrization including ξ_2^\pm as an alternative (but only one $Q = 2$ term at once).

The connection between these anomalous contributions and the underlying instanton-based physical picture can also be derived [30]. It can be shown that $(\det \Phi)^Q$ is generated by multi-instantons with topological charge Q and $(\det \Phi^\dagger)^Q$ by

the corresponding anti-multi-instantons. Generally, higher-order contributions can also be included in \mathcal{L}_{qu} . However, taking dimensional reduction at nonzero temperature as well as parity conservation into account, further $Q \geq 2$ terms are irrelevant.

Note, the term $(\det \Phi^\dagger)^Q$ contains a residual $Z_{(QN_f)}$ symmetry. In particular, the last term of Eq. 1 contains an $Z_2 \times Z_3 \cong Z_6$ symmetry, which is larger than the expected center symmetry Z_3 of the QCD vacuum in the chiral limit. This fact may point to a nonzero contribution of the first (and/or the second) term. Yet, symmetry arguments do not inform us about the relative strength of these contributions.

2.2. Parametrization of the eLSM

In order to correctly implement the axial anomaly in vacuum, at least one of the anomalous couplings $\xi_1, \xi_1^{(1,1)}$, ξ_2, ξ_2^+ , or ξ_2^- has to be nonzero. Hence, if ξ_1 vanishes, the anomaly is encoded in higher-order correlations, as discussed in Ref. [29]. In principle, it would be possible to incorporate temperature- and chemical potential-dependence of these couplings. On the other hand, this would require either additional assumptions on this dependence, or a more advanced, beyond mean-field treatment of the model. In the lack of these, we restrict ourselves to a self-consistent setup with constant parameters.

Following the argument of Ref. [17], one can define an effective anomaly coupling including the contributions of the different terms in Eq. (1). However, in the presence of the $Q = 2$ terms, the leading field dependence cannot be properly factored, and hence different quantities show different relative contributions from these terms. From the expressions for m_π^2 and $m_{\eta_N}^2$ (see the appendix of Ref. [18])—that are distinguished in the model only by the axial anomaly—the effective coupling

$$\xi_{\text{eff}} \equiv \xi_1 + \xi_1^1 (\phi_N^2 + \phi_S^2)/2 + \xi_2 \phi_N^2 \phi_S / \sqrt{2} \quad (3)$$

can be deduced. This is expected to best reflect the relationship between the different couplings, since the $m_\pi^2 - m_{\eta_N}^2$

mass splitting is controlled by the chiral anomaly. Due to the condensate dependence, ξ_{eff} becomes implicitly temperature and chemical potential-dependent. In chiral models, the contribution of the anomaly is always proportional to the—temperature and chemical potential dependent—chiral condensate, in line with general expectations [31].

To determine the model parameters, including each nonzero $\xi_X = \{\xi_1, \xi_1^1, \xi_2, \xi_2^\pm\}$, we fit physical quantities, such as meson masses and decay widths calculated in the model, to their experimental values (for a detailed description and the complete set of quantities see Fit^{1,1,1,2} in Ref. [25]). The parametrization with different combinations of the anomaly terms leads to two important conclusions. First, each combination of terms can provide a fit with a reasonable χ^2 value, hence neither of them can be excluded solely based on vacuum phenomenology. Second, the anomaly-related parameters obey the constraint given by the expectation that only an effective anomaly coupling can be determined, which supports the observation in Ref. [17]. This is shown in Fig. 1, where the best 100 parameter sets are depicted for each setup. Note that in the individual sets the value of ϕ_N and ϕ_S vary, as well as the effective coupling ξ_{eff} might be slightly different. This leads to the fluctuation around the approximate joint surface.

We also note that here we considered not only the case where each coupling is restricted to be nonnegative, but also the general case without such restrictions. While from the point of view of the parametrization the individual sign of the couplings is irrelevant, it turns out that non-negligible negative couplings usually lead to an unstable solution at nonzero T or even in the vacuum ($T = 0$). Therefore, we use only parameter sets that have each $\xi_X > 0$ (circles and triangles in Fig. 1) in the subsequent calculations.

2.3. Extending the anomaly terms within the eLSM: the polydeterminant

A generalization of the determinant appears in effective Lagrangians modelling the chiral anomaly in QCD when different types of mesons are considered [10, 27, 32]. This *polydeterminant* function, also known in the mathematical literature as mixed discriminant, associates N distinct $N \times N$ complex matrices into a complex number and reduces to the usual determinant when all matrices are taken as equal [12].

Given N complex $N \times N$ matrices A_1, A_2, \dots, A_N , the polydeterminant $P\det = \epsilon : \mathbb{C}^{N^2} \rightarrow \mathbb{C}$ reads:

$$\epsilon(A_1, A_2, \dots, A_N) = \frac{1}{N!} \epsilon^{i_1 i_2 \dots i_N} \epsilon^{i'_1 i'_2 \dots i'_N} A_1^{i_1 i'_1} A_2^{i_2 i'_2} \dots A_N^{i_N i'_N}, \quad (4)$$

where $i_k = 1, 2, \dots, N$ and $i'_k = 1, 2, \dots, N$. It is easy to prove that this function is linear and that various properties exist, e.g.: $\epsilon(A, A, \dots, A) = \det(A)$, $\epsilon(A, 1, \dots, 1) = \text{Tr}(A)$, $\epsilon(BA_1, BA_2, \dots, BA_N) = \det(B)\epsilon(A_1, A_2, \dots, A_N)$, etc. We refer to Ref. [12] for a detailed list and related proofs.

In QCD with 3 flavors, one sets $N = N_f = 3$. For instance, if besides the matrix Φ encountered in the previous section we also consider the analogous matrix of

excited (pseudo)scalar meson Φ_E (see Ref. [33] for their phenomenology) the anomalous terms analogous to $\det \Phi$ are:

$$\epsilon(\Phi, \Phi, \Phi_E), \epsilon(\Phi, \Phi_E, \Phi_E), \epsilon(\Phi_E, \Phi_E, \Phi_E) = \det \Phi_E \quad (5)$$

Under chiral transformation $\Phi \rightarrow U_L \Phi U_R^\dagger$, $\Phi_E \rightarrow U_L \Phi_E U_R^\dagger$, thus these terms are chirally symmetry but $U(1)_A$ violating. Such terms were not yet investigated in a quantitative way: this is left for the future.

One may also consider chiral multiplets with nonzero spin. Again, one should consider heterochiral multiplets, that is chiral multiplets transforming as $\Phi \rightarrow U_L \Phi U_R^\dagger$, see the classification in Refs. [10, 27]. Two examples are given by the heterochiral (pseudo)vector mesons Φ_μ (involving the 1^{-+} pseudovector, such as the state $b_1(1235)$ and their flavor and chiral partner, the 1^{--} radially excited vector mesons, such as $\rho(1700)$ [34]), and by the heterochiral pseudotensor mesons $\Phi_{\mu\nu}$ (involving 2^{-+} states such as $\pi_2(1880)$ [35]). Due to the chiral transformations $\Phi_\mu \rightarrow U_L \Phi_\mu U_R^\dagger$ and $\Phi_{\mu\nu} \rightarrow U_L \Phi_{\mu\nu} U_R^\dagger$, Lorentz-invariant chirally symmetric but anomalous interactions take the form

$$\epsilon(\Phi, \Phi_\mu, \Phi^\mu), \epsilon(\Phi, \Phi_{\mu\nu}, \Phi^{\mu\nu}), \dots \quad (6)$$

Mixing patterns in the isoscalar sector (formally similar to the famous mixing leading to $\eta(547)$ and $\eta'(958)$) and specific decay channels follow from such interactions. The strength of these interaction terms can be estimated using a dilute instanton gas, in a way similar to the pseudoscalar case, see Ref. [32].

Summarizing, the polydeterminant allows to introduce novel chirally anomalous interaction terms among different types of mesons, thus allowing the extension of chiral models in general and the eLSM in particular along unexplored directions.

3. The Columbia plot

After carrying out the vacuum study in Sec. 2.2, viable sets of parameters regarding vacuum phenomenology are available, and the resulting phase transition can be explored. We solve the field equations at nonzero T to obtain the chiral condensates $\phi_{N,S}$ and hence determine the order of the phase transition. Repeating this procedure at different values of the explicit symmetry-breaking parameters, h_N and h_S we can draw the Columbia plot within our model.

The square mass of the pion $m_\pi^2 = Z_\pi h_N / \phi_N$ suggests that h_N is proportional to the bare quark mass $m_n = (m_u + m_d)/2$. Similarly, $h_S \propto m_S$. Yet, assuming a strict simple proportionality is valid only at leading order. In fact, the parameters of the low energy model can be extracted by integrating out the fluctuation between $\Lambda_{\text{UV}} \gg 1 \text{ GeV}$, a fixed high-energy scale in the perturbative regime where the masses are fixed, and $\Lambda_{\text{eLSM}} \lesssim 1 - 2 \text{ GeV}$, which is the upper scale of validity of the model [36–38]. The different quark masses at Λ_{UV} lead to different values for all model parameters, not only for h_N and h_S . At the physical

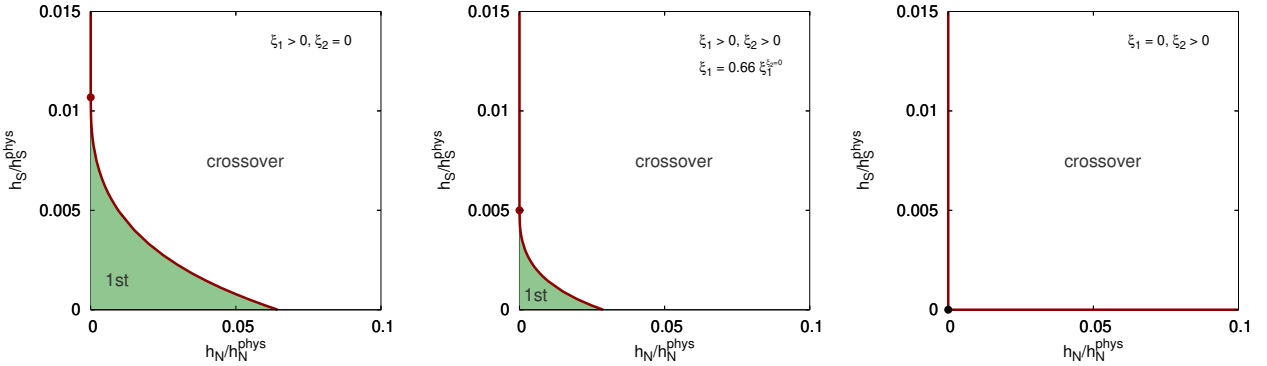


Figure 2: The Columbia plot in the plane of the normalized explicit symmetry breaking parameters with parameters including ξ_1 (left), ξ_2 (right), and both (center).

point, these parameters can be determined by comparing to experimentally measured hadron properties, which we discussed in the previous section. However, as we move away from the critical point by changing $m_{u,d}$ and m_s , the model parameters modify in a nontrivial way.

A large- N_c analysis [39, 40] may help to clarify the issue above and to present a concrete example. The scaling $h_N \sim N_c^{1/2}$ is required, which can be obtained by modifying the ESB as [41]:

$$\mathcal{L}_{\text{ESB}} = \lambda G^2 \text{tr}(M\Phi), \quad (7)$$

where G is the glueball/dilaton field and $M = \text{diag}(m_u, m_d, m_s)$ contains the bare quark masses. The parameter $\lambda \sim N_c^{-3/2}$ because it describes a glueball-glueball- $q\bar{q}$ interaction. Then, in the isospin-symmetric limit, the parameter $h_N = \lambda m_n G_0^2$ correctly scales as $N_c^{1/2}$, but the minimum of the dilaton field G_0 is also dependent on m_n [24]. We may conclude that $h_N = m_n f(m_n, m_s) = m_n f(0, 0) + \dots$. Thus, only at leading order, h_N is simply proportional to m_n .

A full treatment of this problem—similar to that in chiral perturbation theory [15, 42] to circumvent the lack of fundamental QCD input—would be extremely complicated in the eLSM, and is beyond the scope of the present work¹. Therefore, we concentrate on the scenario where only h_N and h_S are varied without mapping them exactly to $m_{u,d}$ and m_s . At leading order and for the qualitative purposes of this work, this is sufficient to derive the Columbia plot.

In Fig. 2 we show the resulting Columbia plots for three different, representative parameter sets. Note that we only show results with varying ξ_1 and ξ_2 , while keeping $\xi_1^{(1,1)} = 0$. Contrary to Ref. [18], we use h_S/h_S^{phys} and h_N/h_N^{phys} instead of m_K and m_π , which causes a deformation of the phase structure for $h_S > 0$ that is presented here.

The left panel shows the Columbia plot where the anomaly is implemented only with the conventional 't Hooft determinant, i.e., $\xi_1 = \bar{\xi}_1 > 0$ and $\xi_2 = 0$. This is in qualitative agreement with other mean-field results where

the anomaly is implemented in the same way, e.g., [15]. In the $h_N = 0$ chiral limit, and physical strange quark mass, $h_S = h_S^{\text{phys}}$, we find a second-order transition. This extends towards smaller h_S until it ends in a tricritical point. Below this point, an extended region where the chiral transition is of first order is found. Starting from the tricritical point, a second-order transition continues with decreasing h_S and increasing h_N until it ends at $h_S = 0$ and $h_N > 0$. For $h_N = 0$ and even larger h_S , only a crossover is found. This is consistent with the expectation for the one-flavor limit, which is reached for $h_S = 0$, $h_N \rightarrow \infty$. In this case, ξ_1 explicitly breaks chiral symmetry, leading to a nonzero chiral condensate for all temperatures.

When $\xi_2 > 0$ is considered, the tricritical point on the left edge moves to lower h_S values. Consequently, the first-order region near the $N_f = 3$ chiral limit shrinks as ξ_2 is increasing and—due to ξ_{eff} being approximately constant among the parametrisations— ξ_1 is decreasing. This is shown in the center panel, where $\xi_1 = 0.66 \bar{\xi}_1$ is used. As ξ_1 further decreases, the first-order region shrinks and disappears at $\xi_1 = 0$, as can be seen on the right panel. In this scenario, the transition becomes second-order also in the $h_N > 0$, $h_S = 0$ chiral limit, and the Columbia plot at $h_N \geq 0$ and $h_S \geq 0$ resembles that in the complete absence of the $U(1)_A$ anomaly. Hence, only from this picture, the $\xi_{\text{eff}} \propto \xi_2$ and the $\xi_{\text{eff}} = 0$ cases cannot be distinguished. Interestingly, this second-order line at $\xi_1 = 0$, $h_S = 0$ is continuously connected to the second-order line at $\xi_1 > 0$, $h_S > 0$, just as the specially symmetric point at $h_S = h_N = 0$ is connected to the tricritical point. Since the presence of the first-order region is favored only in the case of $\xi_1 > 0$ (each ξ_2 , ξ_2^\pm , and ξ_1^1 suppresses this region), it can be concluded that the relative strength of the 't Hooft coupling ξ_1/ξ_{eff} governs the size of this region. In light of recent lattice results, this suggests that the ξ_1 term might not be the dominant contribution for the axial anomaly. Yet, if we insist that the center symmetry should not be larger than Z_3 , the parameter ξ_1 should not vanish: an eventually small but nonzero first-order region is still present in the left-down part of the Columbia plot.

¹For completeness and safety, we restrict our parameters to provide a description qualitatively compatible with chiral perturbation theory results.

Finally, we note that at $h_S < 0$, which was already partially presented in the $m_K \ll m_\pi$ region in Ref. [18], the phase structure is more complicated, possibly including CP-violating phases. This interesting region will be discussed in a future publication.

4. Conclusions

In this work, we reported on some features related to the chiral anomaly, both in vacuum and in the medium. For the ground-state (pseudo)scalar sector, we included terms proportional to the standard 't Hooft determinant term(s) generated by instantons with topological charge one, and to the square of the determinant, which emerges from instantons with topological charge 2. Both terms are consistent with vacuum phenomenology (Fig. 1). This additional term turns out to be important when studying the Columbia plot at nonzero temperature [18]. In particular, the first-order region in the low-left corner of the diagram shrinks when this term dominates (Fig. 2).

When other chiral multiplets are considered, an analogous anomalous 't Hooft term can be introduced by using an extension of the determinant, the so-called polydeterminant [12, 27, 32]. A new class of interaction is possible, whose detailed study represents an outlook of this work.

Acknowledgement The authors thank M. Stephanov for useful discussions. P. K. and G. K. acknowledge support by the Hungarian National Research, Development and Innovation Fund under Project No. K 138277. The work of G. K. is partially supported by the Polish National Science Centre (NCN) under OPUS Grant No. 2022/45/B/ST2/01527.

References

- [1] G. 't Hooft, Phys. Rev. Lett. **37**, 8 (1976).
- [2] G. 't Hooft, Phys. Rept. **142**, 357 (1986).
- [3] R. D. Pisarski and F. Wilczek, Phys. Rev. D **29**, 338 (1984).
- [4] D. J. Gross, S. B. Treiman, and F. Wilczek, Phys. Rev. D **19**, 2188 (1979).
- [5] H. Adhikary *et al.* (NA61/SHINE), Nature Commun. **16**, 2849 (2025), arXiv:2312.06572 [nucl-ex].
- [6] W. Brylinski, M. Gazdzicki, F. Giacosa, M. Gorenstein, R. Poberezhnyuk, S. Samanta, and H. Stroebel, (2023), arXiv:2312.07176 [nucl-th].
- [7] C. Rosenzweig, A. Salomone, and J. Schechter, Phys. Rev. D **24**, 2545 (1981).
- [8] E. Witten, Annals Phys. **128**, 363 (1980).
- [9] D. Parganlija, P. Kovacs, G. Wolf, F. Giacosa, and D. H. Rischke, Phys. Rev. D **87**, 014011 (2013), arXiv:1208.0585 [hep-ph].
- [10] F. Giacosa, P. Kovacs, and S. Jafarzade, Prog. Part. Nucl. Phys. **143**, 104176 (2025), arXiv:2407.18348 [hep-ph].
- [11] S. Navas *et al.* (Particle Data Group), Phys. Rev. D **110**, 030001 (2024).
- [12] F. Giacosa, M. Zakrzewski, S. Jafarzade, and R. D. Pisarski, Lett. Math. Phys. **115**, 119 (2025), arXiv:2502.15617 [math-ph].
- [13] Y. Aoki, G. Endrodi, Z. Fodor, S. D. Katz, and K. K. Szabo, Nature **443**, 675 (2006), arXiv:hep-lat/0611014 .
- [14] A. Butti, A. Pelissetto, and E. Vicari, JHEP **08**, 029 (2003), arXiv:hep-ph/0307036 .
- [15] S. Resch, F. Rennecke, and B.-J. Schaefer, Phys. Rev. D **99**, 076005 (2019), arXiv:1712.07961 [hep-ph].
- [16] G. Fejos, Phys. Rev. D **105**, L071506 (2022), arXiv:2201.07909 [hep-ph].
- [17] R. D. Pisarski and F. Rennecke, Phys. Rev. Lett. **132**, 251903 (2024), arXiv:2401.06130 [hep-ph].
- [18] F. Giacosa, G. Kovács, P. Kovács, R. D. Pisarski, and F. Rennecke, Phys. Rev. D **111**, 016014 (2025), arXiv:2410.08185 [hep-ph].
- [19] F. Cuteri, O. Philipsen, and A. Sciarra, JHEP **11**, 141 (2021), arXiv:2107.12739 [hep-lat].
- [20] A. Bazavov, H. T. Ding, P. Hegde, F. Karsch, E. Laermann, S. Mukherjee, P. Petreczky, and C. Schmidt, Phys. Rev. D **95**, 074505 (2017), arXiv:1701.03548 [hep-lat].
- [21] Y. Kuramashi, Y. Nakamura, H. Ohno, and S. Takeda, Phys. Rev. D **101**, 054509 (2020), arXiv:2001.04398 [hep-lat].
- [22] L. Dini, P. Hegde, F. Karsch, A. Lahiri, C. Schmidt, and S. Sharma, Phys. Rev. D **105**, 034510 (2022), arXiv:2111.12599 [hep-lat].
- [23] J. Bernhardt and C. S. Fischer, Phys. Rev. D **108**, 114018 (2023), arXiv:2309.06737 [hep-ph].
- [24] S. Janowski, F. Giacosa, and D. H. Rischke, Phys. Rev. D **90**, 114005 (2014), arXiv:1408.4921 [hep-ph].
- [25] P. Kovács, Z. Szép, and G. Wolf, Phys. Rev. D **93**, 114014 (2016), arXiv:1601.05291 [hep-ph].
- [26] G. Kovács, P. Kovács, and Z. Szép, Phys. Rev. D **104**, 056013 (2021), arXiv:2105.12689 [hep-ph].
- [27] F. Giacosa, A. Koenigstein, and R. D. Pisarski, Phys. Rev. D **97**, 091901 (2018), arXiv:1709.07454 [hep-ph].
- [28] G. 't Hooft, Phys. Rev. D **14**, 3432 (1976), [Erratum: Phys. Rev. D **18**, 2199 (1978)].
- [29] R. D. Pisarski and F. Rennecke, Phys. Rev. D **101**, 114019 (2020), arXiv:1910.14052 [hep-ph].
- [30] F. Rennecke, Phys. Rev. Res. **2**, 033359 (2020), arXiv:2003.13876 [hep-th].
- [31] Y. Kwon, S. H. Lee, K. Morita, and G. Wolf, Phys. Rev. D **86**, 034014 (2012), arXiv:1203.6740 [nucl-th].
- [32] F. Giacosa, S. Jafarzade, and R. D. Pisarski, Phys. Rev. D **109**, L071502 (2024), arXiv:2309.00086 [hep-ph].
- [33] D. Parganlija and F. Giacosa, Eur. Phys. J. C **77**, 450 (2017), arXiv:1612.09218 [hep-ph].
- [34] M. Piotrowska, C. Reisinger, and F. Giacosa, Phys. Rev. D **96**, 054033 (2017), arXiv:1708.02593 [hep-ph].
- [35] A. Koenigstein and F. Giacosa, Eur. Phys. J. A **52**, 356 (2016), arXiv:1608.08777 [hep-ph].
- [36] F. Rennecke, *The Chiral Phase Transition of QCD.*, Ph.D. thesis, U. Heidelberg (main) (2015).
- [37] P. Springer, J. Braun, S. Rechenberger, and F. Rennecke, EPJ Web Conf. **137**, 03022 (2017), arXiv:1611.06020 [hep-ph].
- [38] W.-j. Fu, J. M. Pawłowski, and F. Rennecke, Phys. Rev. D **101**, 054032 (2020), arXiv:1909.02991 [hep-ph].
- [39] G. 't Hooft, Nucl. Phys. B **72**, 461 (1974).
- [40] E. Witten, Nucl. Phys. B **160**, 57 (1979).
- [41] F. Giacosa, Acta Phys. Polon. B **55**, 4 (2024), arXiv:2402.14097 [hep-ph].
- [42] T. Herpay, A. Patkos, Z. Szep, and P. Szefalussy, Phys. Rev. D **71**, 125017 (2005), arXiv:hep-ph/0504167 .